PHILOSOPHICAL TRANSACTIONS A

rsta.royalsocietypublishing.org

Opinion piece

Cite this article: Kim J, Lee N, Hyeon T. 2017 Recent development of nanoparticles for molecular imaging. *Phil. Trans. R. Soc. A* **375**: 20170022.
http://dx.doi.org/10.1098/rsta.2017.0022

Accepted: 22 April 2017

One contribution of 10 to a discussion meeting issue 'Challenges for chemistry in molecular imaging'.

Subject Areas:
nanotechnology, materials science, biomedical engineering

Keywords:
nanoparticle, molecular imaging, contrast agent

Authors for correspondence:
Nohyun Lee
e-mail: nohyunlee@kookmin.ac.kr
Taeghwan Hyeon
e-mail: thyeon@snu.ac.kr

THE ROYAL SOCIETY PUBLISHING

Recent development of nanoparticles for molecular imaging

Jonghoon Kim[1,2], Nohyun Lee[3] and Taeghwan Hyeon[1,2]

[1]Center for Nanoparticle Research, Institute for Basic Science (IBS), Seoul 08826, Republic of Korea
[2]School of Chemical and Biological Engineering, and Institute of Chemical Processes, Seoul National University, Seoul 08826, Republic of Korea
[3]School of Advanced Materials Engineering, Kookmin University, Seoul 02707, Republic of Korea

TH, 0000-0001-5959-6257

Molecular imaging enables us to non-invasively visualize cellular functions and biological processes in living subjects, allowing accurate diagnosis of diseases at early stages. For successful molecular imaging, a suitable contrast agent with high sensitivity is required. To date, various nanoparticles have been developed as contrast agents for medical imaging modalities. In comparison with conventional probes, nanoparticles offer several advantages, including controllable physical properties, facile surface modification and long circulation time. In addition, they can be integrated with various combinations for multimodal imaging and therapy. In this opinion piece, we highlight recent advances and future perspectives of nanomaterials for molecular imaging.

This article is part of the themed issue 'Challenges for chemistry in molecular imaging'.

1. Introduction

Molecular imaging, which refers to quantitative, non-invasive and repetitive imaging of targeted biomolecules and monitoring of related biological processes in living subjects, has recently attracted much attention of many researchers and clinicians in various fields. It has traditionally been categorized into two groups. The first group includes medical imaging modalities such as magnetic resonance imaging (MRI), computed tomography (CT) and ultrasound imaging, which

can provide anatomical information. The other group includes positron emission tomography (PET), single photon emission CT (SPECT) and optical imaging, which can provide functional or molecular information. However, recent development in contrast agents and imaging techniques allows MRI and CT to be used in molecular imaging. The cellular functions and corresponding molecular processes could be visualized by molecular imaging [1]. Furthermore, owing to the non-invasiveness of molecular imaging, these processes can be monitored in real-time manner. Thus, molecular imaging helps diagnosis of various diseases, prediction of their prognosis and decision on suitable treatment. However, although molecular imaging has enormous potential, the concentration of most target molecules is very low. In addition, there are several intrinsic limitations of imaging modalities, including poor sensitivity (for MRI and CT), low spatial resolution (for PET), and limited penetration depth (for fluorescence imaging). Therefore, a probe with high sensitivity is required for successful imaging. To date, many researchers have reported breakthrough results in molecular imaging using nanoparticles to address these obstacles.

Owing to recent development of targeted contrast agents, including nanoparticles [2], iodinated molecules [3], Gd chelates [4] and fluorescent dyes [5], specific biomarkers can be imaged using the conventional imaging modalities. Among them, nanoparticles emerged as powerful tools for molecular imaging due to their intrinsic unique magnetic or optical properties, which allows their applications to various imaging modalities, and due to long circulation time, which is advantageous for targeted delivery. Nanoparticle generally refers to a particle with a size ranging from 1 to 100 nm. Indeed, these nanostructured materials have a long history of use as contrast agents in various imaging modalities and drug delivery vehicles. Representatively, iron oxide nanoparticles have been applied as contrast agents for MRI, and their contrast effects have been improved by varying the size and composition of the nanoparticles [6,7]. Semiconductor nanoparticles (quantum dots (QDs)) and upconversion nanoparticles (UCNPs) have been used as fluorescent probes in optical imaging due to their high quantum yield and excellent photostability compared with organic dyes [8,9]. Since gold nanoparticles and tantalum oxide nanoparticles have higher X-ray attenuation coefficient than iodinated molecules, they have been developed as CT contrast agents [10,11].

To employ nanoparticles in molecular imaging, a suitable targeting ligand should be conjugated onto the surface of the nanoparticles. Because surface modification of the nanoparticles has been well developed, various targeting molecules, including antibodies, peptides and aptamers, can be readily attached using conventional bioconjugation chemistry. The targeted nanomaterials generally exhibit higher affinity to biomolecules or cells because multiple targeting ligands can be conjugated [12]. Furthermore, the function of the nanoparticles can be expanded by incorporation of various functional materials [13]. The resulting multifunctional nanoparticles enable multimodal imaging and therapy simultaneously, which is referred to as theranosis [14]. Recently, there have been numerous research activities to develop multifunctional nanomaterials to treat various diseases. The multifunctional nanomaterials are expected to lead to precise diagnosis via multimodal imaging and patient-tailored therapy by providing molecular information.

To date, various kinds of nanomaterials, such as dendrimers, liposomes, micelles and inorganic nanoparticles, have been studied for molecular imaging. For nanomaterials based on organic molecules, there are a number of excellent reviews to which the reader may refer, and this opinion piece focuses on the inorganic nanoparticles [15–17]. Herein, we firstly discuss recent efforts in nanotechnology to develop inorganic contrast agents in each imaging modality. Then, we cover several examples of multifunctional nanomaterials for multimodal imaging and theranosis. Finally, we address the future perspectives of nanomaterials in biomedicine.

2. Development of nanoparticles for molecular imaging

For molecular imaging, it is prerequisite to develop a suitable contrast agent with high sensitivity. Enormous progress in nanotechnology has allowed fine control of size, composition and other properties of nanoparticles. As a result, nanoparticles can show outstanding performance in

Table 1. Characteristic of various imaging modalities.

imaging modality	spatial resolution	sensitivity	penetration depth	imaging probe
MRI	∼100 µm	mM–µM	no limit	para-/superpara-/ferromagnetic materials
CT	∼100 µm	>mM	no limit	high-*Z* elements (I, Ba, Au, Bi, Ta, La)
optical imaging	∼a few mm (*in vivo*) sub ∼ µm (*in vitro*)	nM–pM	<1 cm	fluorescent dyes, quantum dots, upconverting nanoparticle
PET	∼a few mm	pM	no limit	radionuclides (^{18}F, ^{11}C, ^{64}Cu, ^{124}I)

molecular imaging. Because the basic principles of medical imaging modalities are different, we will highlight recent advances of nanoparticles for each modality in this section. Table 1 summarizes and compares the characteristics of four representative imaging modalities, namely MRI, CT, optical imaging and PET.

(a) Nanoparticles for magnetic resonance imaging

MRI is one of the most powerful imaging tools in molecular imaging because it is a non-invasive modality providing anatomical, physiological and molecular information within living subjects. It has mainly been adapted for imaging the major organs including the brain and other parts of the central nervous system, for assessing the function of organs such as the heart and kidneys, and for detecting tumours. Owing to high resolution, unlimited penetration depth and excellent soft tissue contrast, MRI is expected to emerge as an important tool for molecular and cellular imaging. Although MRI is mainly used to obtain anatomical information about soft tissues, its sensitivity is not sufficient for molecular imaging [18]. The sensitivity of MRI can be improved using a suitable contrast agent, which can modify the relaxation times of water protons. The most commonly available MRI contrast agents are paramagnetic gadolinium complexes, such as gadolinium diethylenetriamine penta-acetic acid (Gd-DTPA). To date, they have been widely used to detect lesions in the brain such as breakage of the blood–brain barrier (BBB), changes in perfusion, vascularity and flow dynamics of the brain [19].

Since gadolinium-based contrast agents have relatively low relaxivity and a high dose of agents is required, they may cause severe side effects such as nephrogenic systemic fibrosis (NSF) [20]. In addition, it is difficult to obtain targeted MR images with high resolution owing to their intrinsic short circulation time. Although this can be overcome by conjugation of gadolinium chelates onto a macromolecule, the unexcreted ions may increase the possibility of side effects [21]. To overcome these limitations of gadolinium-based contrast agents, iron oxide-based nanomaterials have been extensively studied as a safe contrast agent [7]. It is known that administered iron oxide nanoparticles are mainly cleared by macrophages in the reticuloendothelial system (RES) and slowly degraded in lysosomes [22]. The degraded iron ions are stored as ferritin and used in various biological processes such as producing red blood cells. In addition to the excellent biocompatibility, the sensitivity of iron-based nanoparticles is much higher than that of Gd-based complexes. To date, several iron oxide nanoparticles have been approved by the US Food and Drug Administration (FDA). For example, Ferridex was used as a T_2 contrast agent for imaging liver cancer, and Resovist is also used to characterize focal liver lesions in some countries [23]. Ferumoxytol is clinically approved as an MRI contrast agent and for simultaneous treatment of iron deficiency anaemia due to the tendency to be taken up by macrophages [24]. However, the MRI contrast effect of these nanoparticles is far from optimal due to low crystallinity, relatively small size and broad size distribution.

The MRI contrast effect of nanoparticles depends on their magnetic properties, which can be controlled by changing size and composition [6]. For example, when the size of iron oxide nanoparticles is smaller than 3 nm, they exhibit a weak magnetic moment [25] (figure 1*a–c*).

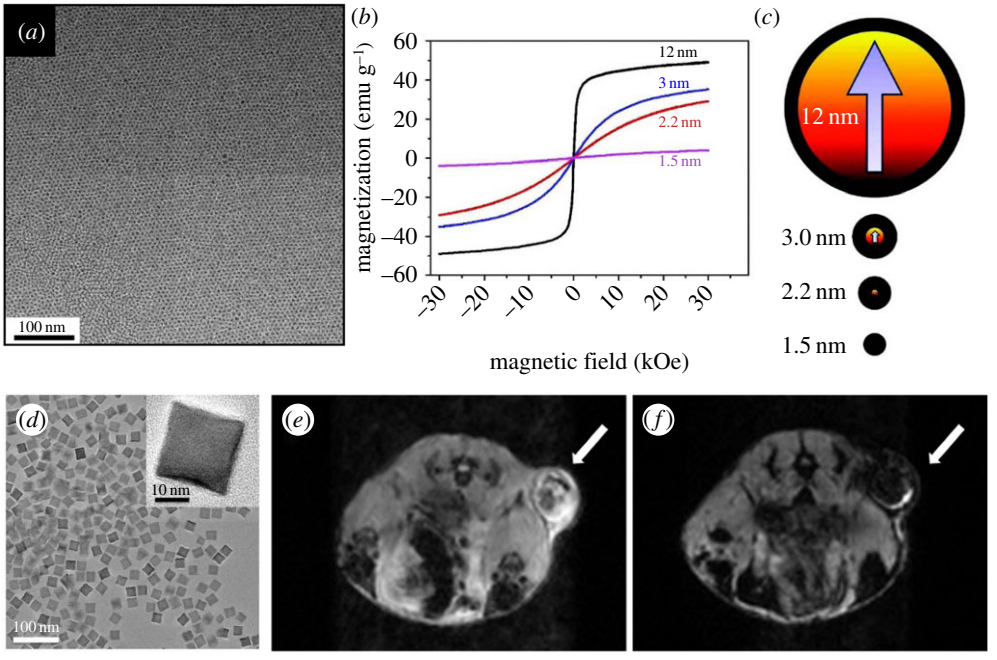

Figure 1. (*a*) Transmission electron microscopy (TEM) image of 3 nm sized ESIONs. (*b*) Field-dependent magnetization curves (*M–H*) at 300 K for various sized iron oxide nanoparticles. (*c*) Illustration of the spin canting effect in various sized iron oxide nanoparticles. Red and black colours represent magnetic cores and magnetically disordered shells. (*d*) TEM image of 22 nm sized FIONs. (*e,f*) *In vivo* MR images of the tumour before (*e*) and 1 h after (*f*) intravenous injection of FIONs. Reproduced with permission from [25] and [27].

Because the magnetic property of extremely small iron oxide nanoparticles (ESIONs) is similar to that of gadolinium complexes, they are appropriate to be used as T_1 contrast agents, exhibiting a low r_2/r_1 ratio. ESIONs are advantageous due to long circulation time, which enables long-term MR imaging with high resolution. It was reported that various kinds of small blood vessels in mouse model were observed using a 3 T MRI scanner, suggesting the feasibility of ESIONs as biocompatible T_1 contrast agents.

When the size of iron oxide nanoparticles exceeds 4 nm, they exhibit saturation magnetization, which increases steeply with their size [26]. Because iron oxide nanoparticles with diameters ranging from 4 to 20 nm do not show any magnetization in the absence of an external magnetic field, they are called superparamagnetic iron oxide (SPIO). If the nanoparticles are larger than 20 nm, residual magnetization exists, which is referred to as ferro-/ferrimagnetic. Since the magnetic field of an MRI scanner is sufficient to saturate the magnetization of nanoparticles, the T_2 contrast effect also increases with their size [26,27]. While the r_1 relaxivity of gadolinium complexes is approximately 4 $mM^{-1}\,s^{-1}$ and r_2 relaxivity of Ferridex is approximately 120 $mM^{-1}\,s^{-1}$, the r_2 relaxivity of ferrimagnetic iron oxide nanoparticles (FIONs) with a size of 22 nm is approximately 750 $mM^{-1}\,s^{-1}$, which is the theoretically estimated maximum r_2 relaxivity of iron oxide nanoparticles. Water-dispersible FIONs can be used for MRI of tumours owing to their long circulation time (figure 1*d–f*).

The MRI contrast effect of nanoparticles can also be modulated by replacing the Fe^{2+} ions at the octahedral sites of inverse spinel structure of Fe_3O_4 with other transition metal ions such as Mn^{2+} and Zn^{2+}. As Mn^{2+} has a similar preference for tetrahedral and octahedral sites, $MnFe_2O_4$ has a mixed spinel structure. The Mn^{2+} doping results in a dramatic effect that $MnFe_2O_4$ nanoparticles exhibit three to six times higher contrast effect than Fe_3O_4 nanoparticles of the same size [28]. Interestingly, because Zn^{2+} ions have a tendency to locate in tetrahedral sites, $Zn_xFe_{2-x}O_4$ has a normal spinel structure exhibiting unique trends of magnetic moments dependent on zinc ratio. The Zn^{2+} ions are initially substituted for Fe^{2+} ions, but

antiferromagnetic interaction of Fe^{3+} at nearby octahedral sites occurs at high Zn doping level. Thus, the net magnetic moment of $Zn_xFe_{2-x}O_4$ nanoparticles reaches a maximum when $x = 0.4$, and the T_2 contrast effect is also highest at this composition [29]. Moreover, the addition of Gd^{3+} ions into iron oxide nanoparticles enhances the T_1 contrast effect owing to the increased interactions between Gd^{3+} ions and water protons [30].

For more accurate diagnosis, it is desirable for the contrast agents to respond to various stimuli such as temperature, pH and enzymes. Although it is shown that conformational changes of Gd complexes in response to stimuli results in T_1 MRI signal alteration [31–33], there are scarce reports on stimuli-responsive contrast agents based on nanoparticles for *in vivo* MRI. The Hyeon group reported that controlled assembly of ESIONs within functional polymers can alter MRI signals [34]. When aggregated, a strong T_2 contrast effect prevents T_1 contrast effect. In acidic condition, ESIONs are disaggregated, and the T_1 contrast effect is recovered, which allows one to diagnose heterogeneous tumours.

(b) Nanoparticles for computed tomography

CT is one of the most commonly used non-invasive imaging modalities due to its high spatial resolution, wide availability, rapid image acquisition and low cost [35]. The imaging principle of CT is based on X-ray attenuation of human body or contrast agents. An irradiated X-ray beam is absorbed or scattered by the tissues or contrast agents, and the reduced X-ray intensity is measured by a detector at different angles. Reconstruction of X-ray intensity profiles allows one to acquire three-dimensional whole-body images with very high spatial resolution.

However, because X-ray attenuation depends on mass density and atomic number, the sensitivity of CT is so low that subtle changes of soft tissues are almost impossible to detect. Therefore, contrast agents are essential to acquire high-quality CT images in a region of interest. Barium sulfate suspensions and iodinated compounds are representative CT contrast agents in clinics due to their high atomic numbers [36]. Currently, the usage of barium sulfate suspensions is limited to imaging the gastrointestinal tract via oral administration owing to the inherent toxicity of Ba^{2+} ions. Iodinated compounds, including Iopamidol, and Iodixanol, are used as injectable CT contrast agents. However, the application of the iodinated agents is also limited owing to their short circulation time, high osmolality and high viscosity. In addition, CT can detect at least micromolar concentrations of these contrast agents, which is too high to be used in molecular imaging [18].

To overcome the limitations of current CT contrast agents, nano-sized iodinated contrast agents have been introduced [35]. These include micellar, polymeric and liposomal contrast agents. Because the nano-sized contrast agents can evade renal filtration, they exhibit a long circulation time, which is essential for molecular imaging. However, the K-edge energy level of iodine is much lower than the energy of X-ray photons used in CT [37]. Thus, for more sensitive CT imaging, contrast agents based on heavy elements are required.

Among the high-*Z* elements, gold nanomaterials such as spheres, rods, shells and cages have also been studied due to their excellent biocompatibility and facile synthesis [38,39]. Since the gold nanoparticles have K-edge energy level of 80.7 keV, they generally exhibit better CT contrast effect than iodine-based contrast agents [37]. Furthermore, X-ray attenuation of gold is less affected by environments such as the presence of water and calcium phosphate compared with iodinated contrast agents, because gold interacts mainly with high-energy X-ray photons [40]. Gold nanoparticles with a size of 1.9 nm from Nanoprobes Inc. were initially studied as an X-ray imaging contrast agent [11]. After intravenous administration, the long circulation time and high X-ray attenuation of gold nanoparticles allowed clear imaging of tumour and blood vessels less than 100 µm in diameter. Later, polyethylene glycol (PEG)-coated gold nanoparticles with a size of approximately 30 nm were developed [41] (figure 2*a*). The nanoparticles accumulate in RES-rich organs and provide the delineation between normal liver and hepatoma (figure 2*b*). In addition to spherical gold nanoparticles, various shapes of gold nanomaterials have been proposed for multifunctional CT contrast agents. For instance, gold nanorods can be used as theranostic agents

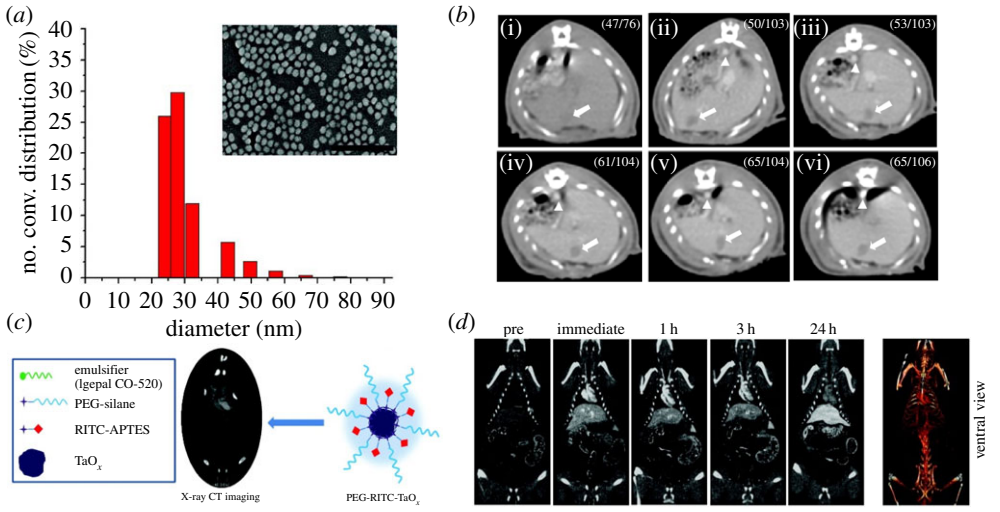

Figure 2. (*a*) Hydrodynamic size distribution and scanning electron microscopy (SEM) image of PEG-coated gold nanoparticles. Scale bar, 300 nm. (*b*) *In vivo* CT serial imaging of a rat hepatoma model before (i) and 5 min (ii), 1 h (iii), 2 h (iv), 4 h (v), 12 h (vi) after intravenous administration of PEG-coated gold nanoparticles. Arrows indicate the hepatoma regions, and arrowheads indicate the aorta. (*c*) Schematic of RITC (rhodamine isothiocyanate)-doped tantalum oxide nanoparticles for X-ray CT imaging. (*d*) *In vivo* CT serial imaging of a rat after intravenous injection of RITC-doped tantalum oxide nanoparticles. Reproduced with permission from [41] and [10].

for simultaneous photothermal therapy (PTT) and CT due to their strong extinction in the near-infrared (NIR) region [42]. In addition, there have been efforts to develop multifunctional CT contrast agents via conjugating various functional molecules such as targeting ligands, peptides and Raman reporters on the gold nanomaterials [2,43].

Although gold nanomaterials are attractive materials as CT contrast agents, they are too expensive to be used in clinics. In fact, approximately 50 g of gold should be consumed for a human whole-body scanning session, making it hard to be commercialized in the market [37]. Thus, there have been attempts to find other cheaper alternatives. For example, lanthanides have been proposed as CT contrast agents because gadolinium complexes have been used as MRI contrast agents in clinics [36]. However, the lanthanide-based molecules exhibit a short circulation time, which prevents targeted imaging. Subsequently, to increase circulation time, macromolecule-conjugated lanthanide chelates have been studied [44]. Dysprosium-DTPA-dextran with a size of approximately 10 nm enables enhanced CT imaging of liver tumours and blood vessels. In addition, emulsions containing lanthanide ions and lanthanide-based inorganic nanoparticles have also been investigated as multifunctional CT contrast agents [45,46].

Tantalum is one of the ideal elements as CT contrast agents owing to its high biocompatibility and radiopacity. In clinics, tantalum-based stents and implants are used frequently. Tantalum oxide nanoparticles can be prepared via sol–gel reaction of tantalum ethoxide followed by facile functionalization with various silane agents [10,47] (figure 2*c*). Because the synthetic procedure of tantalum oxide nanoparticles is similar to that of silica nanoparticles, various multifunctional nanomaterials can be prepared. For instance, PEG-coated tantalum oxide nanoparticles exhibit very long circulation time (figure 2*d*). In addition to tantalum, bismuth- or tungsten-based nanoparticles were also studied as nano-sized CT contrast agents [48,49]. Although further study on the long-term effects of these nanomaterials is required for clinical translation, it is expected that they can overcome the limitation of currently available iodine-based CT contrast agents.

(c) Nanoparticles for optical imaging

Compared with MRI and CT imaging, optical imaging is rapid, inexpensive and sensitive. While whole-body imaging modalities such as MRI and PET have limited temporal and

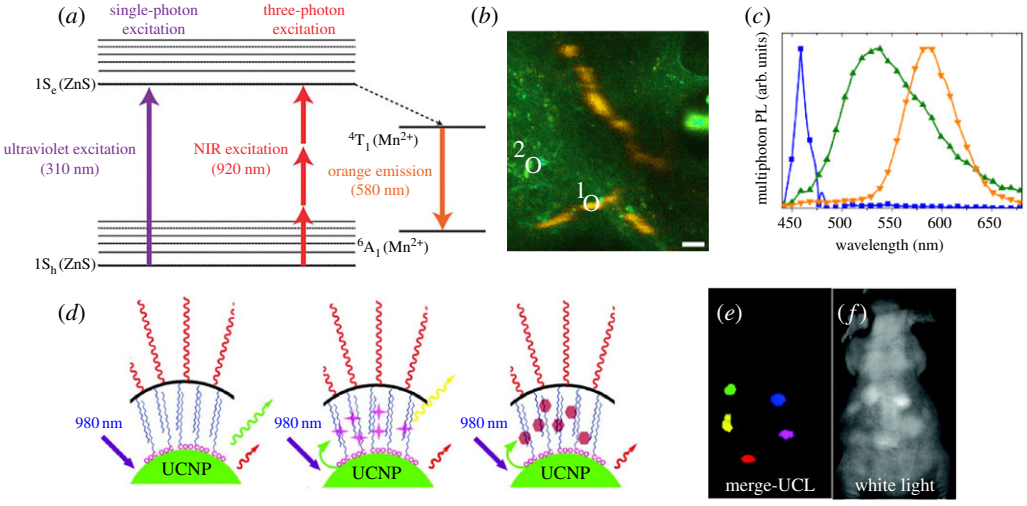

Figure 3. (*a*) Jablonski diagram of one- and three-photon-excited luminescence in nanoparticles. (*b*) Spectral image of tumour vasculature below the dermis after intravenous injection of ZnS:Mn nanoparticles. (*c*) Normalized spectra of three-photon-excited photoluminescence of nanoparticles (orange, region 1 in *b*), tissue autofluorescence (green, region 2 in *b*) and second-harmonic generation from collagen fibre (blue). (*d*) A scheme of UCNPs for multicolour luminescence imaging. (*e*,*f*) *In vivo* multicolour-merged upconversion luminescence image (*e*) and white light image (*f*). Reproduced with permission from [8] and [61].

spatial resolution, optical imaging can provide real-time images with high resolution. Since subcellular phenomena can be captured only by optical microscopy, optical imaging has been vigorously studied to understand the behaviour of various nanomaterials in living subjects [50]. For instance, optical imaging enables one to observe the interactions between nanoparticles and various kinds of cells, including immune cells [51]. Currently, various fluorescent dyes are extensively used as optical imaging probes. However, *in vivo* optical imaging has been hampered by short penetration depth in tissue and background signals caused by light scattering. Many advances of optical imaging probes and techniques have been made to maximize penetration depths and minimize background signals by employing NIR light and/or anti-Stokes imaging [52]. Furthermore, photobleaching and the limited absorption coefficient of fluorescent dyes can also be overcome by developing nanoparticle-based optical probes.

QDs represent various kinds of fluorescent semiconductor nanoparticles exhibiting unique optical and electronic properties that differ from those of their bulk states due to the quantum confinement effect [53]. Their emission wavelength can be easily tuned by varying their size. They exhibit excellent optical characteristics including high quantum yield, absorption coefficient and photostability, enabling long-term fluorescence imaging without photobleaching. Furthermore, the high multi-photon absorption coefficient of QDs allows high-resolution fluorescence imaging by reducing out-of-focus excitation. However, because the initially developed QDs contain toxic elements such as cadmium, there have been great concerns about their safety [54]. To address this issue, cadmium-free QDs have been developed as non-toxic fluorescence probes. For example, manganese-doped ZnS (ZnS:Mn) nanoparticles have been exploited in multi-photon fluorescence imaging [8] (figure 3*a*). The large three-photon cross-section of ZnS:Mn allows high-resolution *in vivo* tumour-targeted imaging because of the deep tissue penetration of 920 nm NIR laser light (figure 3*b*). To further enhance penetration depth, the second near-infrared (NIR-II) region (1000–1700 nm) has also been studied as an optical window. To date, QDs, such as Ag_2S and Ag_2Se, and carbon nanotubes have been applied for NIR-II imaging through a single-photon process [55–57].

Although the aforementioned multi-photon imaging has enormous potential, its efficiency is generally low because it depends on a virtual intermediate state. In this regard, UCNPs are attractive luminescence imaging probes owing to their high efficiency [58]. Upconversion is a unique mechanism of the anti-Stokes emission processes, where multiple low-energy photons are absorbed through a real electronic intermediate state, and subsequently a high-energy photon is emitted. Owing to its high efficiency, a UCNP does not require a high-power pulsed laser. In addition, light scattered by tissue can be removed using time-gated imaging because of the long luminescence lifetime [59]. While the wavelength of QDs depends on their size, the optical properties of UCNPs is dependent on the energy levels of individual lanthanide elements. Thus, the emission wavelengths can be tuned by controlling the elemental composition of UCNPs and luminescence resonance energy transfer, allowing multiplex imaging by different emission colours and lifetimes [60,61] (figure 3*d–f*). In addition, as lanthanide materials have been investigated as MRI or CT contrast agents, lanthanide-based UCNPs can be developed as a multimodal imaging agent [9,62]. Thus, their application will be widened in molecular imaging if several issues such as biosafety are clearly addressed.

(d) Nanoparticles for positron emission tomography

Since the 1970s, PET has emerged as a clinical modality with the advantages of extremely high sensitivity, unlimited penetration depth and availability of quantitative analysis [63]. It is based on visualizing and quantifying positron-emitting radionuclides in living subjects. Annihilation of the emitted positron with a nearby electron leads to generation of two 511 keV photons, which can be detected by PET scanners. Positron-emitting isotopes including ^{11}C, ^{13}N, ^{15}O, ^{18}F, ^{44}Sc, ^{62}Cu, ^{64}Cu, ^{68}Ga, ^{72}As, ^{76}Br, ^{82}Rb, ^{86}Y, ^{89}Zr and ^{124}I are routinely used for PET. Since the PET scanner has outstanding sensitivity and photons display excellent tissue-penetrating properties, it is possible to detect even picomolar concentration of isotopes in deep tissues. This distinguished sensitivity allows us to exploit PET to acquire quantitative information about the biodistribution of injected drugs or nanoparticles, and their accumulation at the target site. Thus, PET has been widely used in various fields including oncology [63], atherosclerosis [64] and cell tracking [65]. Unlike other imaging modalities, the role of nanoparticles in PET imaging is marginal because the positron emission and gamma ray generation occur at the atomic level. Thus, most radiolabelled nanoparticles have been developed for the hybrid/multimodal imaging. To overcome the intrinsic limitations such as lack of anatomical information and low resolution, hybrid imaging modalities such as PET/CT and PET/MRI have been developed.

Among the various PET probes, radioisotope-substituted small molecules such as ^{18}F-fluorodeoxyglucose have been used to monitor biological phenomena such as glucose metabolism [66]. On the other hand, metallo-radioisotopes are typically protected by chelates such as 1,4,7,10-tetraazacyclododecane-1,4,7,10-tetraacetric acid (DOTA), 2-[bis[2-[bis(carboxymethyl)amino]ethyl]amino]acetic acid (DTPA) and hydrazinonicotinic acid (HYNIC) [67]. However, detachment of radioisotopes from the chelator can lead to error in imaging. To address this issue, chelator-free syntheses of PET agents have been proposed. One of the radiolabelling synthesis strategies is addition of radioactive precursors during the synthesis of nanoparticles [68]. Although this method gives a very stable PET agent, generation of radioactive waste and long reaction time limit the wide application of this process. Thus, post-synthesis labelling has also been proposed for fast and efficient labelling of various radioisotopes [69,70] (figure 4).

Among various applications of PET with radiolabelled nanoparticles, the quantitative study of tumour-targeted drug delivery is one of the main applications. For instance, the efficacy of tumour-targeting moieties such as arginine–glycine–aspartic acid (RGD) has been investigated via radiolabelled PET probes [71]. Besides, PET imaging has also been employed in studying inflammatory reactions. Despite numerous potential applications of PET imaging, there are still many challenges to be solved, including inherent toxicity of radioisotopes, improved pharmacokinetics and complete clearance from the body.

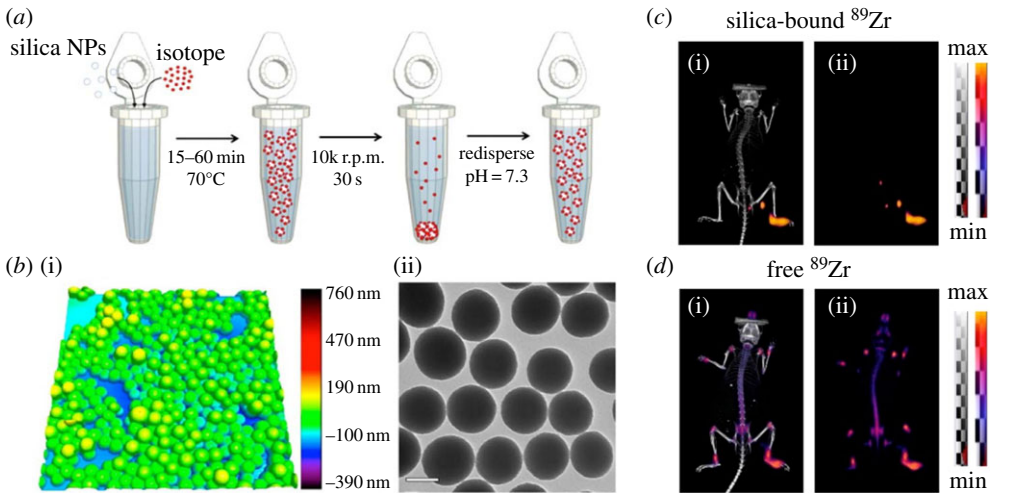

Figure 4. (*a*) Schematic of radiolabelling of silica nanoparticles by post-synthesis labelling method. (*b*) Atomic force microscopy (i) and TEM image (ii) of silica nanoparticles after radiolabelling with ^{68}Ga. Scale bar, 100 nm. (*c*,*d*) *In vivo* PET–CT (i) and PET-only (ii) lymph node imaging 48 h after injection of ^{89}Zr-labelled silica nanoparticles (*c*) and free ^{89}Zr (*d*) in the right rear paw of athymic nude mice. Reproduced with permission from [70].

3. Multifunctional nanoparticles for multimodal molecular imaging and theranosis

Facile modification of nanoparticles allows one to develop multifunctional nanoparticles [13]. While a traditional molecular contrast agent can be detected by a single imaging modality, multifunctional nanoparticles enable multimodal imaging. Simultaneously, the nanoparticles can be used as therapeutic agents via employing their unique physical properties or endowing them with drug delivery capability. Multifunctional nanoparticles not only increase the accuracy of diagnosis but also reduce the side effects of drugs. The multifunctionality can be achieved by combining different types of nanomaterials, functional molecules and targeting agents. In this section, we will briefly introduce several recent examples of multifunctional nanoparticles for multimodal imaging and theranosis.

(a) Nanoparticles for multimodal imaging

Because each imaging modality has its own strengths and weaknesses, multimodal imaging is required to increase the accuracy of diagnosis by obtaining complementary information from each imaging modality. Indeed, some nanoparticles have intrinsic properties suitable for several imaging modalities. For instance, Gd_2O_3 nanoparticles can be used for MRI and CT imaging owing to their high X-ray attenuation coefficient and large number of unpaired electrons of the gadolinium ion [72]. Lanthanide-based UCNPs have been studied for multimodal imaging agents including MRI and optical imaging [73]. The unique optical property of gold nanoparticles allows photoacoustic tomography (PAT) as well as CT [74]. The most general method to prepare multifunctional nanoparticles is the conjugation of functional molecules. For example, iron oxide nanoparticles conjugated with optical or radioisotopes have been exploited for multimodal imaging including MRI/optical imaging or MRI/nuclear imaging [75,76].

The contrast effect can be controlled either by assembly of nanoparticles or by formation of core/shell structures. For example, assembly of multiple iron oxide nanoparticles on the surface of silica nanoparticles enhances the T_2 MRI contrast effect [77]. Although the sensitivity of MRI can be enhanced by contrast agents, it can be affected by several artefacts such as calcification,

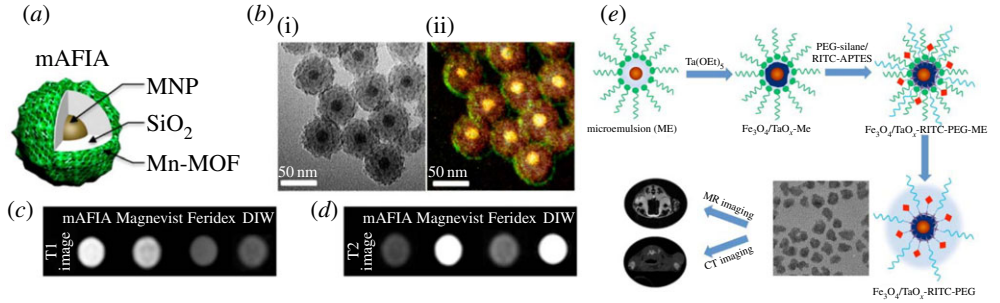

Figure 5. (*a*) Illustration of $Zn_{0.4}Fe_{2.6}O_4$/Mn-MOF core/shell nanoparticle (mAFIA). (*b*) TEM image (i) and energy dispersive X-ray spectroscopy (EDX) analysis of mAFIA (ii). T_1 (*c*) and T_2 (*d*) weighted images of mAFIA compared with conventional MRI contrast agents. (*e*) Schematic illustration of RITC-doped Fe_3O_4/TaO_x core/shell nanoparticle for MRI/CT dual-modal imaging. Reproduced with permission from [78] and [80].

blood clots and air bubbles. However, this can be overcome by self-confirmation using T_1–T_2 dual-mode MRI contrast agents, which can be prepared by controlling the thickness of the silica layer between the magnetic nanoparticle and the paramagnetic shell [78] (figure 5*a–d*).

Since each imaging modality has different sensitivity, the ratio of related contrast agents should be optimized so that they can be detected by any modality. This is critical when preparing contrast agents for CT, which requires very high dose. For example, gadolinium complexes can be used for MRI and CT. However, because too high concentration of T_1 contrast agent suppresses its contrast effect, simultaneous imaging of MRI and CT using gadolinium chelates is almost impossible [79]. To address this limitation, Fe_3O_4/TaO_x core/shell nanoparticles and gold nanoparticles coated with gadolinium chelates are proposed [80,81] (figure 5*e*). These multifunctional imaging agents clearly delineate tumour-associated vessels and tumour microenvironment.

(b) Nanoparticles for theranosis

While traditional imaging and therapeutic agents generally perform a single role, synergistically integrated nanoparticles can be used for simultaneous therapy and diagnosis [14]. There are two approaches for therapeutic applications of nanoparticles. The first is to use intrinsic properties of nanoparticles. For example, magnetic nanoparticles generate heat under an alternating external magnetic field to induce cell death, referred to as magnetic hyperthermia [82]. On the other hand, gold nanostructures including gold nanorods [42], nanoshells [83] and nanocages [84] are employed in PTT, which involves NIR irradiation to induce thermal damage to tumour cells [85] (figure 6*a–c*). The efficiency of magnetic hyperthermia is significantly enhanced by controlling the size, composition and structure of nanoparticles [86]. Apart from gold nanoparticles, various nanomaterials such as carbon nanotubes [87], graphene [88] and CuS [89] nanoparticles can efficiently convert absorbed NIR light into heat. In addition to heat generation, carbon- or titania-based nanomaterials can generate reactive oxygen species (ROS), which destroy cancer cells and blood vessels around a tumour [90–92] (figure 6*d–g*).

The second approach is to use nanoparticles as delivery vehicles. Owing to their long circulation time and targeting capability, nanoparticles increase delivery efficiency and decrease the side effects of the free drug such as non-specific distribution. Nanoparticles can be developed as a delivery carrier simply by conjugation of therapeutic agents on the surface of the nanoparticles. For example, QD-aptamer-doxorubicin conjugates are used for intracellular drug delivery and synchronous fluorescence imaging [93]. To increase the therapeutic effect, cleavable linkers such as disulfide bond are often used [94]. However, because the conjugated molecules are exposed, they can be degraded prior to reaching the target site. Because pores can protect the therapeutic cargoes, mesoporous silica nanoparticles with high porosity and large surface area have been used as a drug delivery vehicle [95]. Owing to facile functionalization with

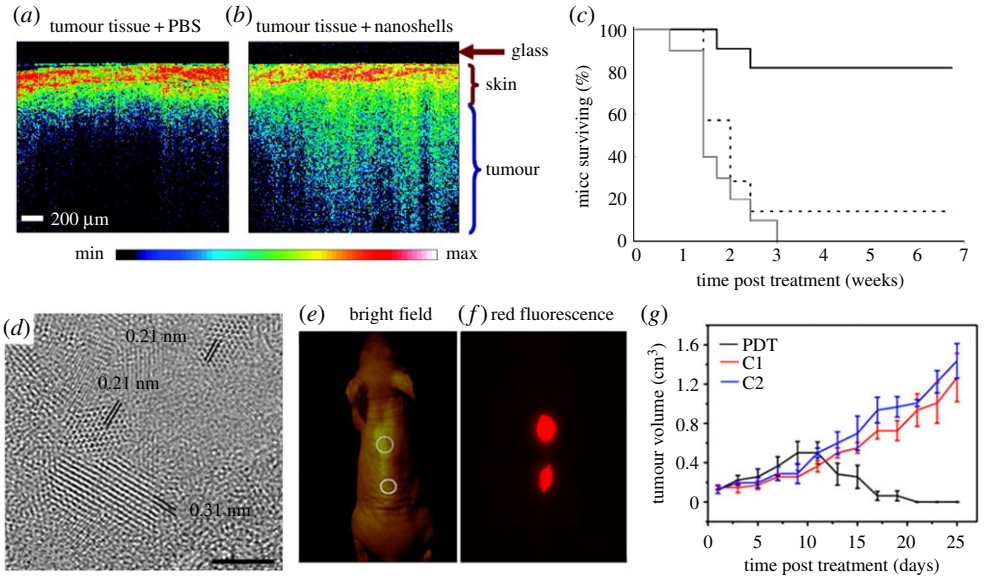

Figure 6. Optical coherence tomography (OCT) images from tumours of mice intravenously administered with phosphate buffered saline (PBS) (*a*) or gold nanoshells (*b*). (*c*) Survival data from the treated groups of gold nanoshell + NIR irradiation (solid black line), PBS sham + NIR laser treatment (dashed black line), untreated control (grey line). (*d*) High-resolution TEM image of graphene quantum dots (GQDs). Scale bar, 2 nm. (*e*,*f*) Bright-field image (*e*) and red-fluorescence image (*f*) after subcutaneous injection of GQDs in different areas (ex/em = 502–540/695–775). (*g*) Time-dependent tumour growth curves ($n = 5$) after PDT treatment compared with control groups (C1, not irradiated group; C2, not GQD-administered group). Reproduced with permission from [85] and [92].

silane agents, various functional moieties including fluorescent dyes and nanoparticles are readily incorporated into the mesoporous silica nanoparticles. For example, core/shell nanoparticles, which are composed of a single iron oxide nanoparticle core and a dye-doped mesoporous silica shell, have been used not only as magnetic resonance and fluorescence imaging agents, but also as a drug delivery vehicle [96]. In addition, drug release can be controlled either via grafting stimuli-responsive functional groups or via inducing supramolecular change of gatekeeper groups [97]. In addition to mesoporous silica nanoparticles, polymers have been developed as delivery carriers for a long time. Although the polymer itself does not have imaging capability, incorporation of nanoparticles allows one to monitor its delivery. Since a number of nanoparticles prepared via thermal decomposition method are hydrophobic, they can be easily incorporated within hydrophobic polymers such as poly(lactic-*co*-glycolic) acid (PLGA) [98].

These two approaches are sometimes combined, resulting in synergetic therapeutic effect. For example, photodynamic therapy (PDT) uses light-sensitive photosensitizers to generate ROS. However, most photosensitizers absorb visible light, but its penetration depth is limited. Because nanoparticles can emit visible light through a multi-photon or upconversion process, a deep penetrating NIR light can be used in PDT [9]. In addition, mild heat generation by nanoparticles increases permeability of tumour vessels, which also enhances the delivery efficiency of drugs [99].

4. Conclusion and outlook

Over the past few years, molecular imaging has been used for many clinical purposes, including quantitative and non-invasive disease diagnosis, disease staging, and visualization and quantification of biological processes. Since each imaging modality has its own pros and cons, combining different imaging modalities enables more accurate diagnosis. Using the various

imaging modalities, early-stage diagnosis, prognosis and even therapeutics of various diseases are readily possible. Nanotechnology has had a lot of influence on molecular imaging as a tool kit, providing additional functionality such as detailed molecular information. Various kinds of functional nanomaterials have been investigated for molecular imaging applications. The novel properties of nanoparticles enable molecular imaging to have high resolution and sensitivity. Compared with small molecule-based contrast agents, nanoparticles exhibit excellent biodistribution, long circulation time and other various functions. Furthermore, multifunctional nanomaterials can serve as multimodal imaging agents or theranostic agents.

Nevertheless, clinical translation of nanomaterials has been much slower than that of small molecule-based materials. Many critical challenges, including toxicity, biocompatibility, targeting efficacy and long-term stability of nanoparticles, should be addressed for their clinical translation. Above all, long-term toxicological studies of nanomaterials in large animal models are highly desirable. Since non-human primates exhibit a high degree of similarity to humans in morphology, physiological function and genetic characteristics, they are expected to play a significant role in evaluating suitability of nanomaterials for biomedical application. Unprecedented side effects on non-human primates after administration of nanomaterials should be investigated before their clinical translation. Moreover, it is also important to choose the most suitable nanomaterials and imaging modalities to obtain desired information. If necessary, multimodal imaging and theranosis should be employed by combining different kinds of nanomaterials. The sustainable development of nanotechnology in molecular imaging is expected to drive the next generation of diagnosis and therapy of diseases in the future.

Data accessibility. This article has no supporting data.

Authors' contributions. J.K., N.L. and T.H. wrote this paper.

Competing interests. The authors have no competing interests.

Funding. T.H. is supported by the Research Center Program of the Institute for Basic Science (IBS) in Korea (IBS-R006-D1). N.L. is supported by the Marine Biotechnology Program (20150220) funded by the Ministry of Oceans and Fisheries, Basic Science Research Program (2015R1C1A1A01053463) and Foreign Research Institute Recruitment Program (2013K1A4A3055679) through the National Research Foundation of Korea (NRF) funded by the Ministry of Science, ICT & Future Planning.

References

1. Jokerst JV, Gambhir SS. 2011 Molecular imaging with theranostic nanoparticles. *Acc. Chem. Res.* **44**, 1050–1060. (doi:10.1021/ar200106e)
2. Kircher MF *et al.* 2012 A brain tumor molecular imaging strategy using a new triple-modality MRI-photoacoustic-Raman nanoparticle. *Nat. Med.* **18**, 829–834. (doi:10.1038/nm.2721)
3. Hyafil F *et al.* 2007 Noninvasive detection of macrophages using a nanoparticulate contrast agent for computed tomography. *Nat. Med.* **13**, 636–641. (doi:10.1038/nm1571)
4. Ye D, Shuhendler AJ, Pandit P, Brewer KD, Tee SS, Cui L, Tikhomirov G, Rutt B, Rao J. 2014 Caspase-responsive smart gadolinium-based contrast agent for magnetic resonance imaging of drug-induced apoptosis. *Chem. Sci.* **5**, 3845–3852. (doi:10.1039/C4SC01392A)
5. Zhu S *et al.* 2017 Molecular imaging of biological systems with a clickable dye in the broad 800- to 1,700-nm near-infrared window. *Proc. Natl Acad. Sci. USA* **114**, 962–967. (doi:10.1073/pnas.1617990114)
6. Lee N, Hyeon T. 2012 Designed synthesis of uniformly sized iron oxide nanoparticles for efficient magnetic resonance imaging contrast agents. *Chem. Soc. Rev.* **41**, 2575–2589. (doi:10.1039/c1cs15248c)
7. Lee N, Yoo D, Ling D, Cho MH, Hyeon T, Cheon, J. 2015 Iron oxide based nanoparticles for multimodal imaging and magnetoresponsive therapy. *Chem. Rev.* **115**, 10 637–10 689. (doi:10.1021/acs.chemrev.5b00112)
8. Yu JH *et al.* 2013 High-resolution three-photon biomedical imaging using doped ZnS nanocrystals. *Nat. Mater.* **12**, 359–366. (doi:doi/10.1038/nmat3565)
9. Park YI *et al.* 2012 Theranostic probe based on lanthanide-doped nanoparticles for simultaneous *in vivo* dual-modal imaging and photodynamic therapy. *Adv. Mater.* **24**, 5755–5761. (doi:10.1002/adma.201202433)

10. Oh MH *et al.* 2011 Large-scale synthesis of bioinert tantalum oxide nanoparticles for X-ray computed tomography imaging and bimodal image-guided sentinel lymph node mapping. *J. Am. Chem. Soc.* **133**, 5508–5515. (doi:10.1021/ja200120k)
11. Hainfeld JF, Slatkin DN, Focella TM, Smilowitz HM. 2006 Gold nanoparticles: a new X-ray contrast agent. *Br. J. Radiol.* **79**, 248–253. (doi:10.1259/bjr/13169882)
12. Jiang W, Kim BYS, Rutka JT, Chan WCW. 2008 Nanoparticle-mediated cellular response is size-dependent. *Nat. Nanotechnol.* **3**, 145–150. (doi:10.1038/nnano.2008.30)
13. Lee JE, Lee N, Kim T, Kim J, Hyeon T. 2011 Multifunctional mesoporous silica nanocomposite nanoparticles for theranostic applications. *Acc. Chem. Res.* **44**, 893–902. (doi:10.1021/ar2000259)
14. Lee D-E, Koo H, Sun I-C, Ryu JH, Kim K, Kwon IC. 2012 Multifunctional nanoparticles for multimodal imaging and theragnosis. *Chem. Soc. Rev.* **41**, 2656–2672. (doi:10.1039/c2cs15261d)
15. Kunjachan S, Ehling J, Storm G, Kiessling F, Lammers, T. 2015 Noninvasive imaging of nanomedicines and nanotheranostics: principles, progress, and prospects. *Chem. Rev.* **115**, 10 907–10 937. (doi:10.1021/cr500314d)
16. Mulder WJM, Strijkers GJ, van Tilborg GAF, Griffioen AW, Nicolay K. 2006 Lipid-based nanoparticles for contrast-enhanced MRI and molecular imaging. *NMR Biomed.* **19**, 142–164. (doi:10.1002/nbm.1011)
17. Cai W, Chen X. 2007 Nanoplatforms for targeted molecular imaging in living subjects. *Small* **3**, 1840–1854. (doi:10.1002/smll.200700351)
18. Willmann JK, Van Bruggen N, Dinkelborg LM, Gambhir SS. 2008 Molecular imaging in drug development. *Nat. Rev. Drug Discov.* **7**, 591–607. (doi:10.1038/nrd2290)
19. Yang C-T, Chuang K-H. 2012 Gd(III) chelates for MRI contrast agents: from high relaxivity to 'smart', from blood pool to blood–brain barrier permeable. *Med. Chem. Commun.* **3**, 552–565. (doi:10.1039/C2MD00279E)
20. Perazella MA. 2009 Current status of gadolinium toxicity in patients with kidney disease. *Clin. J. Am. Soc. Nephrol.* **4**, 461–469. (doi:10.2215/CJN.06011108)
21. Boros E, Gale EM, Caravan P. 2015 MR imaging probes: design and applications. *Dalton Trans.* **44**, 4804–4818. (doi:10.1039/c4dt02958e)
22. Feliu N *et al.* 2016 *In vivo* degeneration and the fate of inorganic nanoparticles. *Chem. Soc. Rev.* **45**, 2440–2457. (doi:10.1039/c5cs00699f)
23. Achilefu S. 2010 Introduction to concepts and strategies for molecular imaging. *Chem. Rev.* **110**, 2575–2578. (doi:10.1021/cr1001113)
24. Lu M, Cohen MH, Rieves D, Pazdur R. 2010 FDA report: ferumoxytol for intravenous iron therapy in adult patients with chronic kidney disease. *Am. J. Hematol.* **85**, 315–319. (doi:10.1002/ajh.21656)
25. Kim BH *et al.* 2011 Large-scale synthesis of uniform and extremely small-sized iron oxide nanoparticles for high-resolution T_1 magnetic resonance imaging contrast agents. *J. Am. Chem. Soc.* **133**, 12 624–12 631. (doi:10.1021/ja203340u)
26. Jun YW *et al.* 2005 Nanoscale size effect of magnetic nanocrystals and their utilization for cancer diagnosis via magnetic resonance imaging. *J. Am. Chem. Soc.* **127**, 5732–5733. (doi:10.1021/ja0422155)
27. Lee N, Choi Y, Lee Y, Park M, Moon WK, Choi SH, Hyeon T. 2012 Water-dispersible ferrimagnetic iron oxide nanocubes with extremely high r_2 relaxivity for highly sensitive *in vivo* MRI of tumors. *Nano Lett.* **12**, 3127–3131. (doi:10.1021/nl3010308)
28. Lee J-H *et al.* 2007 Artificially engineered magnetic nanoparticles for ultra-sensitive molecular imaging. *Nat. Med.* **13**, 95–99. (doi:10.1038/nm1467)
29. Jang J-T, Nah H, Lee J-H, Moon SH, Kim MG, Cheon J. 2009 Critical enhancements of MRI contrast and hyperthermic effects by dopant-controlled magnetic nanoparticles. *Angew. Chem. Int. Edn.* **48**, 1234–1238. (doi:10.1002/anie.200805149)
30. Zhou Z *et al.* 2013 Engineered iron-oxide-based nanoparticles as enhanced T_1 contrast agents for efficient tumor imaging. *ACS Nano* **7**, 3287–3296. (doi:10.1021/nn305991e)
31. Lubag AJM, De Leon-Rodriguez LM, Burgess SC, Sherry AD. 2011 Noninvasive MRI of β-cell function using a Zn^{2+}-responsive contrast agent. *Proc. Natl Acad. Sci. USA* **108**, 18 400–18 405. (doi:10.1073/pnas.1109649108)
32. De Leon-Rodriguez LM, Lubag AJM, Malloy CR, Martinez GV, Gillies RJ, Sherry AD. 2009 Responsive MRI agents for sensing metabolism *in vivo*. *Acc. Chem. Res.* **42**, 948–957. (doi:10.1021/ar800237f)

33. Gianolio E, Stefania R, Di Gregorio E, Aime S. 2012 MRI paramagnetic probes for cellular labeling. *Eur. J. Inorg. Chem.* **2012**, 1934–1944. (doi:10.1002/ejic.201101399)
34. Ling D *et al.* 2014 Multifunctional tumor pH-sensitive self-assembled nanoparticles for bimodal imaging and treatment of resistant heterogeneous tumors. *J. Am. Chem. Soc.* **136**, 5647–5655. (doi:10.1021/ja4108287)
35. Lee N, Choi SH, Hyeon T. 2013 Nano-sized CT contrast agents. *Adv. Mater.* **25**, 2641–2660. (doi:10.1002/adma.201300081)
36. Yu S-B, Watson AD. 1999 Metal-based X-ray contrast media. *Chem. Rev.* **99**, 2353–2378. (doi:10.1021/cr980441p)
37. FitzGerald PF, Colborn RE, Edic PM, Lambert JW, Torres AS, Bonitatibus JPJ, Yeh BM. 2016 CT image contrast of high-Z elements: phantom imaging studies and clinical implications. *Radiology* **278**, 723–733. (doi:10.1148/radiol.2015150577)
38. Dreaden EC, Alkilany AM, Huang X, Murphy CJ, El-Sayed MA. 2012 The golden age: gold nanoparticles for biomedicine. *Chem. Soc. Rev.* **41**, 2740–2779. (doi:10.1039/c1cs15237h)
39. Xi D, Dong S, Meng X, Lu Q, Meng L, Ye J. 2012 Gold nanoparticles as computerized tomography (CT) contrast agents. *RSC Adv.* **2**, 12 515–12 524. (doi:10.1039/C2RA21263C)
40. Galper MW, Saung MT, Fuster V, Roessl E, Thran A, Proksa R, Fayad ZA, Cormode DP. 2012 Effect of computed tomography scanning parameters on gold nanoparticle and iodine contrast. *Invest. Radiol.* **47**, 475–481. (doi:10.1097/RLI.0b013e3182562ab9)
41. Kim D, Park S, Lee JH, Jeong YY, Jon S. 2007 Antibiofouling polymer-coated gold nanoparticles as a contrast agent for *in vivo* x-ray computed tomography imaging. *J. Am. Chem. Soc.* **129**, 7661–7665. (doi:10.1021/ja071471p)
42. von Maltzahn G, Park J-H, Agrawal A, Bandaru NK, Das SK, Sailor MJ, Bhatia SN. 2009 Computationally guided photothermal tumor therapy using long-circulating gold nanorod antennas. *Cancer Res.* **69**, 3892–3900. (doi:10.1158/0008-5472.CAN-08-4242)
43. Popovtzer R, Agrawal A, Kotov NA, Popovtzer A, Balter J, Carey TE, Kopelman R. 2008 Targeted gold nanoparticles enable molecular CT imaging of cancer. *Nano Lett.* **8**, 4593–4596. (doi:10.1021/nl8029114)
44. Vera DR, Mattrey RF. 2002 A molecular CT blood pool contrast agent. *Acad. Radiol.* **9**, 784–792. (doi:10.1016/S1076-6332(03)80348-3)
45. Pan D *et al.* 2012 An early investigation of ytterbium nanocolloids for selective and quantitative 'multicolor' spectral CT imaging. *ACS Nano* **6**, 3364–3370. (doi:10.1021/nn300392x)
46. Ni D *et al.* 2016 PEGylated $NaHoF_4$ nanoparticles as contrast agents for both X-ray computed tomography and ultra-high field magnetic resonance imaging. *Biomaterials* **76**, 218–225. (doi:10.1016/j.biomaterials.2015.10.063)
47. Bonitatibus Jr PJ, Torres AS, Goddard GD, FitzGerald PF, Kulkarni AM. 2010 Synthesis, characterization, and computed tomography imaging of a tantalum oxide nanoparticle imaging agent. *Chem. Commun.* **46**, 8956–8958. (doi:10.1039/c0cc03302b)
48. Rabin O, Manuel Perez J, Grimm J, Wojtkiewicz G, Weissleder R. 2006 An X-ray computed tomography imaging agent based on long-circulating bismuth sulphide nanoparticles. *Nat. Mater.* **5**, 118–122. (doi:10.1038/nmat1571)
49. Guo W, Guo C, Zheng N, Sun T, Liu S. 2016 Cs_xWO_3 nanorods coated with polyelectrolyte multilayers as a multifunctional nanomaterial for bimodal imaging-guided photothermal/photodynamic cancer treatment. *Adv. Mater.* **29**, 1604157. (doi:10.1002/adma.201604157)
50. Nam SH, Bae YM, Park YI, Kim JH, Kim HM, Choi JS, Lee KT, Hyeon T, Suh YD. 2011 Long-term real-time tracking of lanthanide ion doped upconverting nanoparticles in living cells. *Angew. Chem. Int. Edn.* **50**, 6093–6097. (doi:10.1002/anie.201007979)
51. Champion JA, Mitragotri S. 2006 Role of target geometry in phagocytosis. *Proc. Natl Acad. Sci. USA* **103**, 4930–4934. (doi:10.1073/pnas.0600997103)
52. Kim D, Lee N, Park YI, Hyeon T. 2017 Recent advances in inorganic nanoparticle-based NIR luminescence imaging: semiconductor nanoparticles and lanthanide nanoparticles. *Bioconjugate Chem.* **28**, 115–123. (doi:10.1021/acs.bioconjchem.6b00654)
53. Medintz IL, Uyeda HT, Goldman ER, Mattoussi H. 2005 Quantum dot bioconjugates for imaging, labelling and sensing. *Nat. Mater.* **4**, 435–446. (doi:10.1038/nmat1390)

54. Tsoi KM, Dai Q, Alman BA, Chan WCW. 2013 Are quantum dots toxic? Exploring the discrepancy between cell culture and animal studies. *Acc. Chem. Res.* **46**, 662–671. (doi:10.1021/ar300040z)
55. Zhang Y, Hong G, Zhang Y, Chen G, Li F, Dai H, Wang Q. 2012 Ag_2S quantum dot: a bright and biocompatible fluorescent nanoprobe in the second near-infrared window. *ACS Nano* **6**, 3695–3702. (doi:10.1021/nn301218z)
56. Dong B, Li C, Chen G, Zhang Y, Zhang Y, Deng M, Wang Q. 2013 Facile synthesis of highly photoluminescent Ag_2Se quantum dots as a new fluorescent probe in the second near-infrared window for *in vivo* imaging. *Chem. Mater.* **25**, 2503–2509. (doi:10.1021/cm400812v)
57. Hong G, Lee JC, Robinson JT, Raaz U, Xie L, Huang NF, Cooke JP, Dai H. 2012 Multifunctional *in vivo* vascular imaging using near-infrared II fluorescence. *Nat. Med.* **18**, 1841–1846. (doi:10.1038/nm.2995)
58. Chatterjee DK, Gnanasammandhan MK, Zhang Y. 2010 Small upconverting fluorescent nanoparticles for biomedical applications. *Small* **6**, 2781–2795. (doi:10.1002/smll.201000418)
59. Zheng X, Zhu X, Lu Y, Zhao J, Feng W, Jia G, Wang F, Li F, Jin D. 2016 High-contrast visualization of upconversion luminescence in mice using time-gating approach. *Anal. Chem.* **88**, 3449–3454. (doi:10.1021/acs.analchem.5b04626)
60. Lu Y *et al.* 2014 Tunable lifetime multiplexing using luminescent nanocrystals. *Nat. Photon.* **8**, 32–36. (doi:10.1038/nphoton.2013.322)
61. Cheng L, Yang K, Shao M, Lee S-T, Liu Z. 2011 Multicolor *in vivo* imaging of upconversion nanoparticles with emissions tuned by luminescence resonance energy transfer. *J. Phys. Chem. C* **115**, 2686–2692. (doi:10.1021/jp111006z)
62. Rieffel J *et al.* 2015 Hexamodal imaging with porphyrin-phospholipid-coated upconversion nanoparticles. *Adv. Mater.* **27**, 1785–1790. (doi:10.1002/adma.201404739)
63. Rohren EM, Turkington TG, Coleman RE. 2004 Clinical applications of PET in oncology. *Radiology* **231**, 305–332. (doi:10.1148/radiol.2312021185)
64. Rudd JHF *et al.* 2008 Atherosclerosis inflammation imaging with ^{18}F-FDG PET: carotid, iliac, and femoral uptake reproducibility, quantification methods, and recommendations. *J. Nucl. Med.* **49**, 871–878. (doi:10.2967/jnumed.107.050294)
65. Doyle B *et al.* 2007 Dynamic tracking during intracoronary injection of ^{18}F-FDG-labeled progenitor cell therapy for acute myocardial infarction. *J. Nucl. Med.* **48**, 1708–1714. (doi:10.2967/jnumed.107.042838)
66. Zhuang H *et al.* 2001 Dual time point ^{18}F-FDG PET imaging for differentiating malignant from inflammatory processes. *J. Nucl. Med.* **42**, 1412–1417. See http://jnm.snmjournals.org/content/42/9/1412.full.
67. Thorp-Greenwood FL, Coogan MP. 2011 Multimodal radio- (PET/SPECT) and fluorescence imaging agents based on metallo-radioisotopes: current applications and prospects for development of new agents. *Dalton Trans.* **40**, 6129–6143. (doi:10.1039/C0DT01398F)
68. Zeng J, Jia B, Qiao R, Wang C, Jing L, Wang F, Gao M. 2014 *In situ* ^{111}In-doping for achieving biocompatible and non-leachable ^{111}In-labeled Fe_3O_4 nanoparticles. *Chem. Commun.* **50**, 2170. (doi:10.1039/c3cc48948e)
69. Chakravarty R, Valdovinos HF, Chen F, Lewis CM, Ellison PA, Luo H, Meyerand ME, Nickles RJ, Cai W. 2014 Intrinsically germanium-69-labeled iron oxide nanoparticles: synthesis and in-vivo dual-modality PET/MR imaging. *Adv. Mater.* **26**, 5119–5123. (doi:10.1002/adma.201401372)
70. Shaffer TM, Wall MA, Harmsen S, Longo VA, Drain CM, Kircher MF, Grimm J. 2015 Silica nanoparticles as substrates for chelator-free labeling of oxophilic radioisotopes. *Nano Lett.* **15**, 864–968. (doi:10.1021/nl503522y)
71. Lee H-Y, Li Z, Chen K, Hsu AR, Xu C, Xie J, Sun S, Chen X. 2008 PET/MRI dual-modality tumor imaging using arginine-glycine-aspartic (RGD)-conjugated radiolabeled iron oxide nanoparticles. *J. Nucl. Med.* **49**, 1371–1379. (doi:10.2967/jnumed.108.051243)
72. Ahmad MW *et al.* 2015 Potential dual imaging nanoparticle: Gd_2O_3 nanoparticle. *Sci. Rep.* **5**, 8549. (doi:10.1038/srep08549)
73. Park YI *et al.* 2009 Nonblinking and nonbleaching upconverting nanoparticles as an optical imaging nanoprobe and T_1 magnetic resonance imaging contrast agent. *Adv. Mater.* **21**, 4467–4471. (doi:10.1002/adma.200901356)

74. Cheng L *et al.* 2014 PEGylated WS_2 nanosheets as a multifunctional theranostic agent for *in vivo* dual-modal CT/photoacoustic imaging guided photothermal therapy. *Adv. Mater.* **26**, 1886–1893. (doi:10.1002/adma.201304497)
75. Xie J, Chen K, Huang J, Lee S, Wang J, Gao J, Li X, Chen X. 2010 PET/NIRF/MRI triple functional iron oxide nanoparticles. *Biomaterials* **31**, 3016–3022. (doi:10.1016/j.biomaterials.2010.01.010)
76. Choi J-S, Park JC, Nah H, Woo S, Oh J, Kim KM, Cheon GJ, Chang Y, Yoo J, Cheon J. 2008 A hybrid nanoparticle probe for dual-modality positron emission tomography and magnetic resonance imaging. *Angew. Chem. Int. Edn.* **47**, 6259–6262. (doi:10.1002/anie.200801369)
77. Lee J-H, Jun Y-W, Yeon S-I, Shin J-S, Cheon J. 2006 Dual-mode nanoparticle probes for high-performance magnetic resonance and fluorescence imaging of neuroblastoma. *Angew. Chem. Int. Edn.* **45**, 8160–8162. (doi:10.1002/anie.200603052)
78. Shin T-H, Choi J-S, Yun S, Kim I-S, Song H-T, Kim Y, Park KI, Cheon J. 2014 T_1 and T_2 dual-mode MRI contrast agent for enhancing accuracy by engineered nanomaterials. *ACS Nano* **8**, 3393–3401. (doi:10.1021/nn405977t)
79. Regino CAS, Walbridge S, Bernardo M, Wong KJ, Johnson D, Lonser R, Oldfield EH, Choyke PL, Brechbiel MW. 2008 A dual CT-MR dendrimer contrast agent as a surrogate marker for convection-enhanced delivery of intracerebral macromolecular therapeutic agents. *Contrast Media Mol. Imaging* **3**, 2–8. (doi:10.1002/cmmi.223)
80. Lee N *et al.* 2012 Multifunctional Fe_3O_4/TaO_x core/shell nanoparticles for simultaneous magnetic resonance imaging and X-ray computed tomography. *J. Am. Chem. Soc.* **134**, 10 309–10 312. (doi:10.1021/ja3016582)
81. Alric C *et al.* 2008 Gadolinium chelate coated gold nanoparticles as contrast agents for both X-ray computed tomography and magnetic resonance imaging. *J. Am. Chem. Soc.* **130**, 5908–5915. (doi:10.1021/ja078176p)
82. Bae KH, Park M, Do MJ, Lee N, Ryu JH, Kim GW, Kim C, Park TG, Hyeon T. 2012 Chitosan oligosaccharide-stabilized ferrimagnetic iron oxide nanocubes for magnetically modulated cancer hyperthermia. *ACS Nano* **6**, 5266–5273. (doi:10.1021/nn301046w)
83. Hirsch LR, Stafford RJ, Bankson JA, Sershen SR, Rivera B, Price RE, Hazle JD, Halas NJ, West JL. 2003 Nanoshell-mediated near-infrared thermal therapy of tumors under magnetic resonance guidance. *Proc. Natl Acad. Sci. USA* **100**, 13 549–13 554. (doi:10.1073/pnas.2232479100)
84. Chen J, Glaus C, Laforest R, Zhang Q, Yang M, Gidding M, Welch MJ, Xia Y. 2010 Gold nanocages as photothermal transducers for cancer treatment. *Small* **6**, 811–817. (doi:10.1002/smll.200902216).
85. Gobin AM, Lee MH, Halas NJ, James WD, Drezek RA, West JL. 2007 Near-infrared resonant nanoshells for combined optical imaging and photothermal cancer therapy. *Nano Lett.* **7**, 1929–1934. (doi:10.1021/nl070610y)
86. Lee J-H *et al.* 2011 Exchange-coupled magnetic nanoparticles for efficient heat induction. *Nat. Nanotechnol.* **6**, 418–422. (doi:10.1038/NNANO.2011.95)
87. Kam NWS, O'Connell M, Wisdom JA, Dai H. 2005 Carbon nanotubes as multifunctional biological transporters and near-infrared agents for selective cancer cell destruction. *Proc. Natl Acad. Sci. USA* **102**, 11 600–11 605. (doi:10.1073/pnas.0502680102)
88. Yang K, Hu L, Ma X, Ye S, Cheng L, Shi X, Li C, Li Y, Liu Z. 2012 Multimodal imaging guided photothermal therapy using functionalized graphene nanosheets anchored with magnetic nanoparticles. *Adv. Mater.* **24**, 1868–1872. (doi:10.1002/adma.201104964)
89. Zhou M, Li J, Liang S, Sood AK, Liang D, Li C. 2015 CuS nanodots with ultrahigh efficient renal clearance for positron emission tomography imaging and image-guided photothermal therapy. *ACS Nano* **9**, 7085–7096. (doi:10.1021/acsnano.5b02635)
90. Huang P *et al.* 2012 Light-triggered theranostics based on photosensitizer-conjugated carbon dots for simultaneous enhanced-fluorescence imaging and photodynamic therapy. *Adv. Mater.* **24**, 5104–5110. (doi:10.1002/adma.201200650)
91. Rehman FU, Zhao C, Jiang H, Wang X. 2016 Biomedical applications of nano-titania in theranostics and photodynamic therapy. *Biomater. Sci.* **4**, 40–54. (doi:10.1039/C5BM00332F)
92. Ge J *et al.* 2014 A graphene quantum dot photodynamic therapy agent with high singlet oxygen generation. *Nat. Commun.* **5**, 4596. (doi:10.1038/ncomms5596)

93. Bagalkot V, Zhang L, Levy-Nissenbaum E, Jon S, Kantoff PW, Langer R, Farokhzad OC. 2007 Quantum dot-aptamer conjugates for synchronous cancer imaging, therapy, and sensing of drug delivery based on bi-fluorescence resonance energy transfer. *Nano Lett.* **7**, 3065–3070. (doi:10.1021/nl071546n)
94. Lee J-H, Lee K, Moon SH, Lee Y, Park TG, Cheon J. 2009 All-in-one target-cell-specific magnetic nanoparticles for simultaneous molecular imaging and siRNA delivery. *Angew. Chem. Int. Edn.* **48**, 4174–4179. (doi:10.1002/anie.200805998)
95. Li Z, Barnes JC, Bosoy A, Stoddart JF, Zink JI. 2012 Mesoporous silica nanoparticles in biomedical applications. *Chem. Soc. Rev.* **41**, 2590–2605. (doi:10.1039/c1cs15246g).
96. Kim J, Kim HS, Lee N, Kim T, Kim H, Yu T, Song IC, Moon WK, Hyeon T. 2008 Multifunctional uniform nanoparticles composed of a magnetite nanocrystal core and a mesoporous silica shell for magnetic resonance and fluorescence imaging and for drug delivery. *Angew. Chem. Int. Edn.* **47**, 8438–8441. (doi:10.1002/anie.200802469)
97. Lee JE, Lee DJ, Lee N, Kim BH, Choi SH, Hyeon T. 2011 Multifunctional mesoporous silica nanocomposite nanoparticles for pH controlled drug release and dual modal imaging. *J. Mater. Chem.* **21**, 16 869–16 872. (doi:10.1039/c1jm11869b)
98. Kim J, Lee JE, Lee SH, Yu JH, Lee JH, Park TG, Hyeon T. 2008 Designed fabrication of a multifunctional polymer nanomedical platform for simultaneous cancer-targeted imaging and magnetically guided drug delivery. *Adv. Mater.* **20**, 478–483. (doi:10.1002/adma.200701726)
99. Kong G, Braun RD, Dewhirst MW. 2001 Characterization of the effect of hyperthermia on nanoparticle extravasation from tumor vasculature. *Cancer Res.* **61**, 3027–3032. See (http://cancerres.aacrjournals.org/content/61/7/3027)